

Two-Photon Photosensitized Production of Singlet Oxygen

Peter K. Frederiksen,[†] Mikkel Jørgensen,[‡] and Peter R. Ogilby^{*,†}

Contribution from the Department of Chemistry, Aarhus University, DK-8000 Aarhus, Denmark, and Condensed Matter Physics and Chemistry Department, Risø National Laboratory, DK-4000 Roskilde, Denmark

Received September 22, 2000. Revised Manuscript Received November 20, 2000

Abstract: Singlet molecular oxygen ($a^1\Delta_g$) has been produced and optically detected upon two-photon nonlinear excitation of a sensitizer with a focused laser beam. The experiments were performed using toluene solutions with either a substituted difuranonaphthalene or a substituted distyryl benzene as the sensitizer. The data indicate that the two-photon absorption cross sections of the difuranonaphthalenes are comparatively large and depend significantly on the functional groups attached to the chromophore. The time-resolved 1270 nm phosphorescence signals used to characterize the production of singlet oxygen are limited in much the same way as signals from other two-photon spectroscopic studies (e.g., weak signals that can be masked by scattered radiation). Nevertheless, the two-photon singlet oxygen signals also reflect the unique advantages of this nonlinear optical technique (e.g., depth penetration in the sample afforded by irradiation in a spectral region void of the more dominant one-photon linear transitions and spatial resolution afforded by irradiation with a focused laser beam).

Introduction

The photosensitized production of singlet molecular oxygen ($a^1\Delta_g$) has important ramifications in disciplines that range from photobiology to polymer science.¹ In the vast literature on singlet oxygen photosensitization, one finds that sensitizer excitation is invariably achieved via a one-photon linear transition between the ground state, S_0 , and a singlet excited state, S_n . Rapid relaxation of the S_n state initially populated yields the lowest excited singlet state of the sensitizer, S_1 . Although ground-state oxygen can quench S_1 of some molecules, singlet oxygen is generally more efficiently generated upon oxygen quenching of the sensitizer triplet state, T_1 , produced upon $S_1 \rightarrow T_1$ intersystem crossing.

In certain molecules, the production of an excited-state singlet can also occur upon the simultaneous absorption of two lower-energy photons.^{2,3} Of particular interest is the case where the transition proceeds via a virtual state, following selection rules that differ from those for a one-photon transition.² A range of phenomena derived from such nonlinear two-photon transitions can be studied using pulsed lasers that deliver high photon intensities.³ Of special interest is the opportunity to selectively excite a two-photon transition at the point of a focused laser beam where a local domain of sufficiently high fluence can be obtained. This aspect of pumping a two-photon transition can be used to impart spatial resolution to an experiment and thus is pertinent, for example, in the construction of emission microscopes.^{4,5} Moreover, irradiation at a wavelength that does not coincide with the dominant one-photon transition facilitates depth penetration in samples that might otherwise be opaque.

This can be important in photodynamic therapy, for example.⁶ Although the use of two-photon nonlinear optical techniques to populate excited electronic states is well established, it has heretofore not been demonstrated as a viable pathway for the photosensitized production of singlet oxygen.

Although the mechanism and selection rules of excited-state population in a two-photon pumping scheme differ from those in a one-photon pumping scheme, and although the initial states populated as a result of these transitions are likewise different, both processes ultimately result in the creation of the lowest excited singlet state, S_1 , via internal conversion. A key difference between these respective processes that, in turn, reflects the respective mechanisms of excitation will be the yield with which this lowest singlet state is produced. In general, the S_1 yield is ~ 7 – 8 orders of magnitude lower for the two-photon process than for the one-photon process.⁷ Nevertheless, once this singlet state is formed, subsequent events such as fluorescence and/or intersystem crossing will be independent of whether a one- or two-photon pumping scheme was used.⁶ Thus, if one is able to (1) overcome the limitations associated with low excited-state yields and the concomitant weak spectroscopic signals and (2) identify a molecule that not only can efficiently produce singlet oxygen but also has an appreciable two-photon absorption cross section, one should, in principle, be able to demonstrate that singlet oxygen can also be formed as a result of a two-photon photosensitized process. We now report that singlet oxygen can, indeed, be produced and optically detected upon two-photon excitation of either a substituted difuranonaphthalene or a substituted distyryl benzene in a focused laser beam. Properties of these molecules pertinent to the photosensitized production of singlet oxygen have also been examined.

* To whom correspondence should be addressed.

[†] Aarhus University.

[‡] Risø National Laboratory.

(1) *Singlet Oxygen*; Frimer, A. A., Ed.; CRC Press: Boca Raton, FL, 1985; Vols. I–IV.

(2) McClain, W. M. *Acc. Chem. Res.* **1974**, *7*, 129–135.

(3) Kershaw, S. In *Characterization Techniques and Tabulations for Organic Nonlinear Optical Materials*; Kuzyk, M. G., Dirk, C. W., Eds.; Marcel Dekker, Inc.: New York, 1998; pp 515–654.

(4) Williams, R. M.; Piston, D. W.; Webb, W. W. *FASEB J.* **1994**, *8*, 804–813.

(5) Xu, C.; Zipfel, W.; Shear, J. B.; Williams, R. M.; Webb, W. W. *Proc. Natl. Acad. Sci. U.S.A.* **1996**, *93*, 10763–10768.

(6) Fisher, W. G.; Partridge, W. P.; Dees, C.; Wachter, E. A. *Photochem. Photobiol.* **1997**, *66*, 141–155.

(7) Fisher, W. G.; Lytle, F. E. *Anal. Chem.* **1993**, *65*, 631–635.

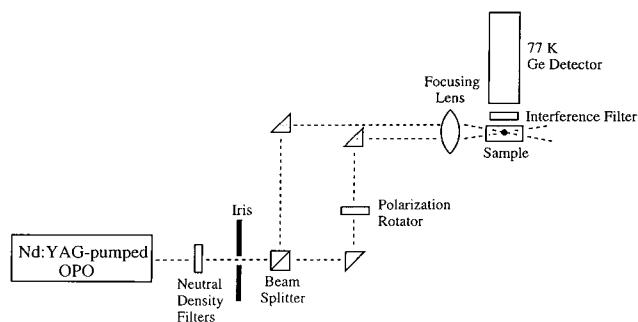


Figure 1. Schematic diagram of the optical layout used for two-photon irradiation.

Experimental Section

Apparatus and Techniques. Although most of the work was done using a nanosecond laser system, a few experiments were performed with a femtosecond system.

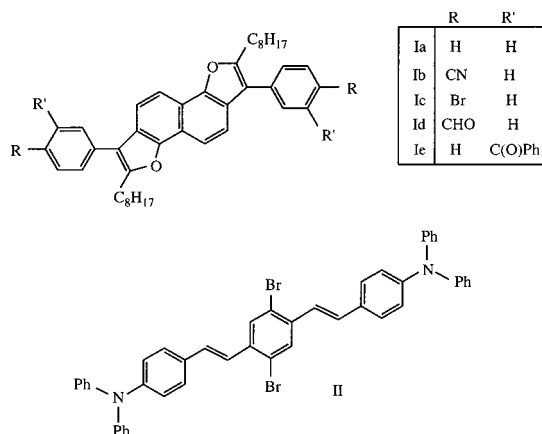
The femtosecond experiments used a regenerative amplified Ti:sapphire system (Clark MXR CPA 1000) operated at a repetition rate of 1 kHz. Samples were irradiated at 802 nm with 90 fs pulses (fwhm) at energies over the range $\sim 1\text{--}50 \mu\text{J/pulse}$. The laser output (~ 2 mm diameter beam) was focused into the center of a 4 cm path length sample cell using a 20 cm focal length lens. Thus, upon entering and exiting the cell, the laser beam had a diameter of $\sim 200 \mu\text{m}$.

The nanosecond experiments were performed using a Nd:YAG-pumped optical parametric oscillator (OPO) as the irradiation source (Quanta-Ray GCR 230 and MOPO 710, pulse fwhm ~ 5 ns, 10 Hz repetition rate). In some of the studies, specific irradiation wavelengths were also obtained by (1) stimulated Raman scattering of the Nd:YAG output in a high-pressure cell of H_2 and (2) frequency doubling of the OPO output. For the one-photon experiments, the sample was irradiated with an unfocused beam ~ 3 mm in diameter using discrete laser wavelengths less than ~ 400 nm. A 1 cm path length cuvette was used for these studies. For the two-photon experiments, discrete laser wavelengths in the range $\sim 590\text{--}880$ nm were used, and the laser output was focused in the sample using a 35 mm focal length lens. Under the latter conditions, which are far from optimal,⁴ a beam width $< 100 \mu\text{m}$ is obtained at the focus. A 4 cm path length cuvette was used for the two-photon studies, and the laser beam focus was centered in this cuvette. The volume of sample used was typically 3 mL. A diagram of the optical layout used for the two-photon experiment is shown in Figure 1. In this case, two optical paths were created using a prism beam-splitter. The polarization of the beam in one path was then chosen to be either parallel or perpendicular to that in the other beam path using a zero-order $\lambda/2$ phase retardation plate (Alphas). The separate beams were then focused into the sample using the same 35 mm focal length lens. We established that, in this configuration, the respective beams properly intersected at the same point in the sample by comparing the intensity of the singlet oxygen phosphorescence signal thus obtained to that observed from a single beam configuration. Specifically, in the two-beam configuration with identical polarization, the signal intensity observed was identical to that observed upon focusing a single beam of comparable energy into the sample.

For the two-photon experiments, the laser intensity, I_L , was varied over the range $\sim 1\text{--}30 \text{ mJ pulse}^{-1} \text{ cm}^{-2}$ using neutral density filters placed in the unfocused beam (~ 3 mm diameter). For the one-photon experiments, I_L was varied by changing the output energy of the flash lamps used to pump the Nd:YAG laser. Laser energies were quantified using volume calorimeters (Scientech).

Singlet oxygen phosphorescence was monitored with a North Coast model EO-817P Ge detector operated at 77 K. The 1270 nm singlet oxygen emission was detected through a silicon window (CVI optics) and an interference filter (Barr Associates, fwhm = 50 nm). Signals were recorded and averaged using a Tektronix model TDS754A digital oscilloscope. Time-resolved absorption measurements were recorded using a 150 W steady-state Xe lamp as the probe source. A chopper (New Focus model 3501) synchronized to the timing of the pulsed excitation laser limited the exposure time of the sample to the broad

Chart 1



band Xe lamp output. Spectral discrimination of the absorption signals was obtained with a Chromex model 250is spectrograph. Signals were monitored with either a gated intensifier/CCD camera (Princeton Instruments) or a photomultiplier tube (Hamamatsu R928).

In the two-photon experiments using the difuranonaphthalenes **Ia–e**, most of the data were recorded using sensitizer concentrations of 2×10^{-3} M in air-saturated toluene. For the experiments in which data from **Id** were compared to data from compound **II**, a concentration of 3×10^{-4} M was used. All of the data on compound **II** were recorded using a concentration of 3×10^{-4} M. In the one-photon experiments, the sensitizer concentration was adjusted to yield a ground-state absorbance of ~ 0.5 at the irradiating wavelength. For all sensitizers, the clear onset of one-photon ground-state absorption (i.e., $A > \sim 0.02$) occurred at wavelengths shorter than ~ 520 nm. Most importantly, for the samples used in the two-photon experiments, measured absorbances were < 0.002 in the range $\sim 550\text{--}800$ nm (note that some light scattering also contributes to the absorbances measured). Absorption spectra were recorded with either a Cary model 17 spectrophotometer or a Hewlett-Packard model 8453 diode array spectrometer.

Sensitizer Preparation. The difuranonaphthalenes **Ia–e** and the distyrylbenzene **II** used as singlet oxygen sensitizers are shown in Chart 1. The syntheses of these compounds are outlined in Schemes 1 and 2. Briefly, K_2CO_3 -promoted substitution of either 1-phenyl-2-bromodecanone or 1-(4-bromophenyl)-2-bromodecanone with 1,5-dihydroxynaphthalene produced the intermediary 1,5-bis(1-arylnon-1-on-2-yloxy)naphthalenes. Treatment of the latter with methanesulfonic acid in methylene chloride yielded the 3,8-diaryl-2,7-dioxydifurano[2,3-*a*:2',3'-*f*]naphthalenes **Ia** and **Ic**, respectively. Compound **Ic** was treated with copper(I) cyanide under Ullman-type conditions to give the dinitrile **Ib**. Alternatively, bromine-to-lithium exchange followed by reaction with dimethylformamide produced the dialdehyde **Id**. Compound **Ie** was prepared from **Ia** by benzylation in a Friedel–Crafts reaction. The meta substitution observed appears to result from prior complexation of the Lewis acid, AlCl_3 , to the oxygen heterocycle. Details of these respective syntheses are provided elsewhere.⁸

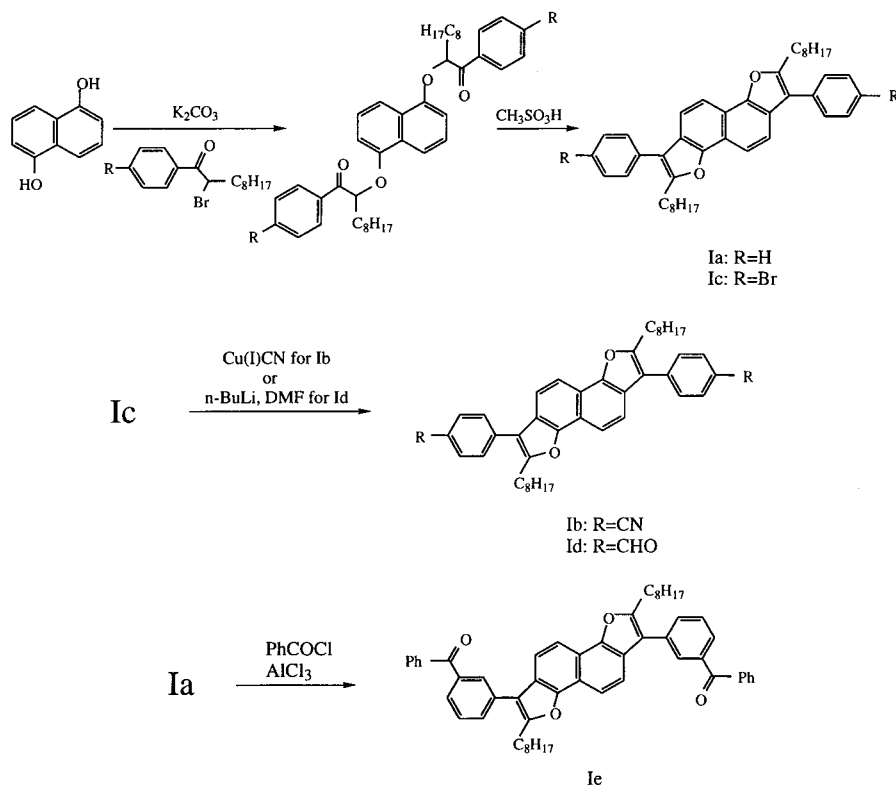
2,5-Bis(4-diphenylaminostyryl)-1,4-dibromobenzene (**II**) was synthesized via a Horner–Wadsworth–Emmons reaction between [2,5-dibromo-4-(diethoxyphosphorylmethyl)benzyl]phosphonic acid diethyl ester and 4-(diphenylamino)benzaldehyde.⁹ The phosphonate ester was prepared from 2,5-dibromo-1,4-xylene,⁹ and the 4-(diphenylamino)benzaldehyde was prepared via formylation of triphenylamine.¹⁰ In the coupling reaction to make **II**, 251 mg (0.47 mmol) of the phosphonate ester and 275 mg (1.0 mmol) of the carboxy triphenylamine were dissolved in 10 mL of DMF under an atmosphere of argon. Potassium *tert*-butylate (200 mg, 1.78 mmol) was added, and the color of the mixture immediately changed from light yellow to dark red, and the orange-yellow product began to precipitate. The reaction mixture was stirred at ambient temperature for 1 h and then diluted with water, and

(8) Jørgensen, M.; Krebs, F. C.; Bechgaard, K. *J. Org. Chem.* **2000**, *65*, 8783–8785.

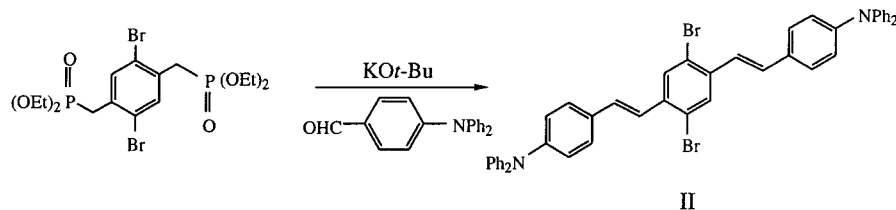
(9) Blum, J.; Zimmerman, M. *Tetrahedron* **1972**, *28*, 275–280.

(10) Baker, T. N.; Doherty, W. P.; Kelley, W. S.; Newmeyer, W.; Rogers, J. E.; Spalding, R. E.; Walter, R. I. *J. Org. Chem.* **1965**, *30*, 3714–3718.

Scheme 1



Scheme 2



the product was filtered. The solid material was recrystallized from benzene to give 240 mg (66% yield) of an orange microcrystalline powder which decomposed at 275 °C. ¹H NMR (CDCl₃, 250.1 MHz) δ: 7.05–7.2 (m, 16H), 7.24–7.38 (m, 12H), 7.45 (d, 4H, *J* = 9 Hz), 7.87 (s, 2H) ppm. ¹³C NMR (CDCl₃, 62.9 MHz) δ: 123.3, 123.5, 123.8, 124.3, 125.2, 128.3, 129.8, 130.4, 130.9, 131.9, 137.7, 147.8, 148.5 ppm.

Results and Discussion

Using guidelines that are available for maximizing two-photon absorption cross sections,^{2,11} we set out to prepare efficient two-photon singlet oxygen sensitizers. The molecules examined in this regard, the difuranonaphthalenes **Ia–e**, are shown in Chart 1. The pendant *n*-octyl moieties were included simply to increase the solubility of these compounds in toluene, the solvent in which our work was done. Albota et al.¹¹ have recently shown that substituted distyryl benzenes can have appreciable two-photon absorption cross sections. Although we have determined that singlet oxygen yields from this general class of molecules can be low upon one-photon irradiation,¹² Albota et al. speculated that one distyryl benzene in particular, the bis-

Table 1. Singlet Oxygen Yields and Two-Photon Cross Sections for Compounds **Ia–d** and **II**^a

sensitizer	one-photon singlet oxygen quantum yield	two-photon absorption cross section at 618 nm ^b (×10 ⁵⁰ cm ⁴ s photon ⁻¹)
Ia	0.36 ± 0.04	8 ± 2
Ib	0.36 ± 0.04	139 ± 35
Ic	0.42 ± 0.05	7 ± 2
Id	0.49 ± 0.06	205 ± 50
II	0.46 ± 0.05	

^a Data recorded in toluene. ^b Obtained by comparing two-photon singlet oxygen phosphorescence intensities, normalized by the one-photon singlet oxygen yield, to the two-photon singlet oxygen phosphorescence intensity from compound **II**, again normalized by the one-photon singlet oxygen yield (see text). The errors shown were obtained by combining our experimental error (~±10%) with the error reported for our reference standard (±15%). Data from **Ia–d** were recorded at 17 mJ pulse⁻¹ cm⁻², whereas data from **II** were recorded at 13 mJ pulse⁻¹ cm⁻².

diphenylamino compound **II** (Chart 1), might, in fact, be a good two-photon singlet oxygen sensitizer. We thus also examined the behavior of **II** as a singlet oxygen sensitizer.

One-Photon Results. We ascertained that **Ia–d** and **II** generate singlet oxygen in appreciable yield upon one-photon excitation (Table 1). In these experiments, the singlet oxygen yields were quantified by comparing the intensity of the 1270 nm singlet oxygen phosphorescence signal obtained upon irradiation of **Ia–d** and **II** to the singlet oxygen signal observed

(11) Albota, M.; Beljonne, D.; Brédas, J.-L.; Ehrlich, J. E.; Fu, J.-Y.; Heikal, A. A.; Hess, S. E.; Kogej, T.; Levin, M. D.; Marder, S. R.; McCord-Maughon, D.; Perry, J. W.; Rockel, H.; Rumi, M.; Subramaniam, G.; Webb, W. W.; Wu, X.-L.; Xu, C. *Science* **1998**, *281*, 1653–1656.

(12) Dam, N.; Scurlock, R. D.; Wang, B.; Ma, L.; Sundahl, M.; Ogilby, P. R. *Chem. Mater.* **1999**, *11*, 1302–1305.

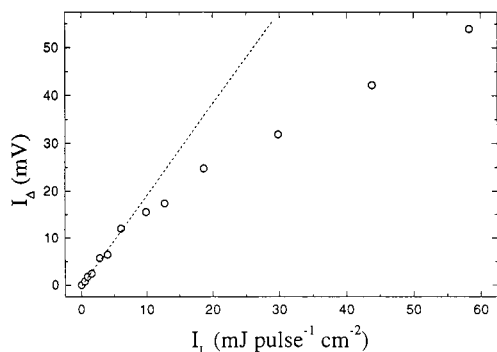


Figure 2. Plot of the singlet oxygen phosphorescence intensity, I_A , against the intensity of the irradiation laser, I_L . Data were recorded upon irradiation of **IIb** in toluene at 355 nm (one-photon pumping scheme). The dashed line results from a linear fit to the first seven data points.

upon irradiation of acridine. Experiments were performed in air-saturated toluene using a reference singlet oxygen quantum yield of 0.83 ± 0.06 for acridine.¹³ Samples were irradiated at 355 nm with energies $< 5 \text{ mJ pulse}^{-1} \text{ cm}^{-2}$, and the data were normalized for the number of photons absorbed by the respective sensitizers.

Upon sensitizer excitation in a one-photon pumping scheme, the intensity of the singlet oxygen signal, I_A , should increase linearly with an increase in the intensity of the pump laser, I_L . Using compound **IIb**, we ascertained that this was, indeed, the case at low laser intensities ($< 7 \text{ mJ pulse}^{-1} \text{ cm}^{-2}$ at 355 nm). At higher laser intensities, however, I_A did not increase as much as expected on the basis of this linear correlation, and plots of I_A against I_L showed curvature concave to the I_L axis (Figure 2). Similar observations have been made for the production of singlet oxygen in other systems.¹⁴ These latter data have been attributed to secondary absorption of light by a sensitizer excited state within the irradiating pulse at high I_L that, in turn, decreases the relative yield of the sensitizer triplet state.¹⁴ Independent transient absorption experiments of our sensitizers support this interpretation. Specifically, upon irradiation of compound **IIb** at 355 nm, we recorded a transient absorption band with a maximum at $\sim 620 \text{ nm}$ that we assign to the **IIb** triplet state on the basis of an oxygen quenching experiment (quenching rate constant $\sim 3 \times 10^9 \text{ s}^{-1} \text{ M}^{-1}$). In plots of this transient absorbance against I_L , the data likewise showed curvature concave to the I_L axis. Moreover, this curvature was identical to that seen in the plots of I_A against I_L , which is to be expected if the sensitizer triplet state is a precursor to singlet oxygen.

Nanosecond Two-Photon Results. Upon irradiation of **Ia–e** at discrete wavelengths over the range $\sim 590\text{--}680 \text{ nm}$ and upon irradiation of **II** at discrete wavelengths over the range $\sim 780\text{--}880 \text{ nm}$, we were able to detect the characteristic time-resolved, 1270 nm singlet oxygen phosphorescence from the laser beam focal point. For compounds **Id** and **II**, singlet oxygen signals could be detected with laser intensities, I_L , as low as $\sim 1 \text{ mJ pulse}^{-1} \text{ cm}^{-2}$. The signal decay was always single exponential, and the singlet oxygen lifetimes obtained were consistent with those expected for experiments performed in toluene.¹⁵ Specif-

ically, upon irradiation of compound **II**, singlet oxygen lifetimes in the range $\sim 27\text{--}29 \mu\text{s}$ were recorded. Upon irradiation of **IIb** and **Id**, slightly shorter lifetimes were obtained ($\sim 18\text{--}20 \mu\text{s}$). The latter data reflect quenching of singlet oxygen by the sensitizer, an observation confirmed in independent one-photon experiments. The singlet oxygen lifetimes observed were independent of I_L over the range $1\text{--}30 \text{ mJ pulse}^{-1} \text{ cm}^{-2}$. Upon prolonged irradiation (i.e., ~ 2000 laser pulses) of **Ia–e** at $10 \text{ mJ pulse}^{-1} \text{ cm}^{-2}$ in an air-saturated solution with the laser focused into a sample volume of 3 mL, the ground-state absorption spectra showed changes that were consistent with the degradation of $\sim 10\%$ of the total amount of sensitizer present in the cuvette.

A number of control experiments were also performed. Specifically, singlet oxygen signals were not observed from sensitizer-free toluene upon irradiation over this same wavelength range of $\sim 590\text{--}880 \text{ nm}$ with a focused laser. We also irradiated two “standard” molecules well known to be efficient one-photon singlet oxygen sensitizers, acridine and pyrene, using a focused laser beam at wavelengths approximately twice those of the corresponding one-photon transitions. Singlet oxygen signals were not observed upon irradiation of pyrene over the range $\sim 600\text{--}670 \text{ nm}$ and of acridine at 683 nm.

For two-photon absorption, I_A should scale according to the square of I_L . Using compound **IIb**, the data, indeed, meet this expectation at low I_L (Figure 3). However, as with the one-photon experiments, the I_A data recorded at higher laser intensities do not increase as much as expected on the basis of this quadratic dependence (Figure 3). On the basis of our one-photon control experiments (vide supra), we infer that this curvature likewise reflects a decrease in the yield of the sensitizer triplet state, T_1 , with an increase in I_L . Specifically, after two-photon excitation, secondary absorption by a sensitizer excited state within the irradiating pulse is presumed to initiate a process that results in a smaller yield of T_1 . This secondary absorption could either be a one- or two-photon transition. Again, because T_1 is the immediate precursor to singlet oxygen, any event that results in a decrease in the T_1 yield will be reflected in the yield of singlet oxygen. In this regard, it is pertinent to note that, in two-photon fluorescence studies, significant deviations from a quadratic dependence on I_L are frequently observed.¹⁶ The latter data have been attributed to a variety of factors, including secondary absorption by an excited state.¹⁶ For our present study, and arguably most importantly, the plot of I_A against I_L shown in Figure 3 indicates that the singlet oxygen data recorded upon $\sim 590\text{--}680 \text{ nm}$ irradiation with a focused laser are certainly not consistent with a one-photon pumping scheme.

Action spectra were recorded for **IIb** and **Id** by plotting I_A , normalized with respect to irradiation intensity, against the irradiation wavelength over the range $590\text{--}670 \text{ nm}$ (Figures 4 and 5). An analogous action spectrum was recorded for **II** over the range $\sim 780\text{--}880 \text{ nm}$ (Figure 6). For **IIb** and **II**, the data show a distinct absorption band at approximately twice the wavelength of the one-photon absorption bands. For **Id**, however, the action spectrum does not reveal such a distinct band over the wavelength range examined. For many molecules, two-photon fluorescence excitation spectra can be recorded and, in turn, can similarly be compared to the one-photon absorption

(13) Wilkinson, F.; Helman, W. P.; Ross, A. B. *J. Phys. Chem. Ref. Data* **1993**, *22*, 113–262.

(14) Gorman, A. A.; Hamblett, I.; Lambert, C.; Prescott, A. L.; Rodgers, M. A. J.; Spence, H. M. *J. Am. Chem. Soc.* **1987**, *109*, 3091–3097.

(15) Wilkinson, F.; Helman, W. P.; Ross, A. B. *J. Phys. Chem. Ref. Data* **1995**, *24*, 663–1021.

(16) Xu, C.; Webb, W. W. In *Topics in Fluorescence Spectroscopy*; Lakowicz, J., Ed.; Plenum Press: New York, 1997; Vol. 5, Nonlinear and Two-Photon-Induced Fluorescence, pp 471–540.

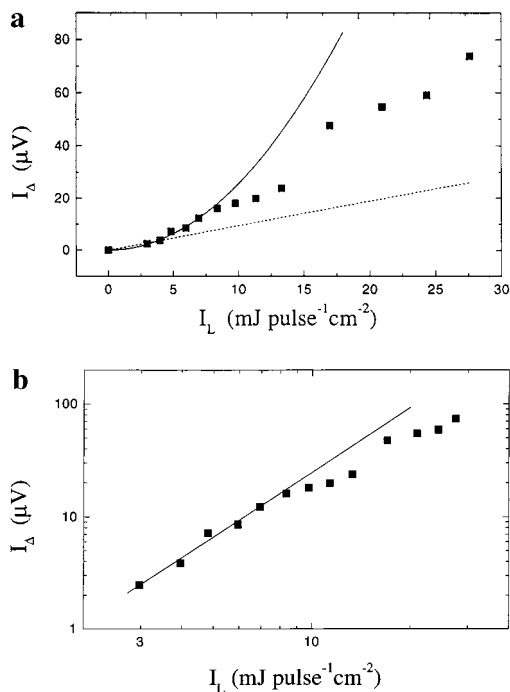


Figure 3. (a) Plot of the singlet oxygen phosphorescence intensity, I_A , against the intensity of the irradiation laser, I_L . Data were recorded upon irradiation of **Ib** in toluene with a focused laser at 618 nm. Functions that illustrate the ideal one-photon (i.e., linear) as well as two-photon (i.e., quadratic) dependence of I_A against I_L are also shown. On the basis of material in Figure 2, plots of I_A against I_L for a one-photon pumping scheme are expected to be linear only at low values of I_L . Thus, to approximate the behavior expected for a one-photon process, a linear fit was applied to the first three data points only (dashed line). The solid line is a quadratic fit to the first six data points. (b) Logarithmic plot of the data shown in (a). The solid line is a linear fit to the first five data points (the 0,0 point in (a) must be excluded from the logarithmic plot) and has a slope of 1.9 ± 0.2 . A slope of 2.0 is expected for a two-photon process.

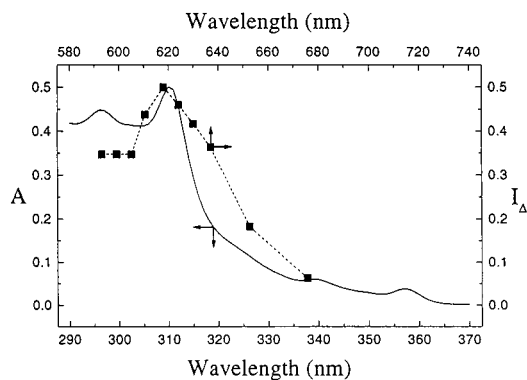


Figure 4. Plot of the normalized singlet oxygen phosphorescence intensity, I_A , against the irradiation wavelength for **Ib** (top and right axes). Superimposed on this plot is the one-photon absorption spectrum of **Ib** (bottom and left axes).

spectra. From such studies, it is clear that, in some cases, the spectral profile of one-photon absorption can differ significantly from that of two-photon absorption at twice the wavelength.^{5,16} Such data are consistent with those of **Id** shown in Figure 5. Nevertheless, there is also ample evidence to indicate that, as with our data from **Ib** and **II**, the one-photon absorption profile can resemble the two-photon profile at twice the wavelength (e.g., fluorescence excitation data recorded for β -naphthol, benzene, toluene, and fluorescein, among other molecules).^{5,7,16–19} Among other things, these differences in two-photon absorption

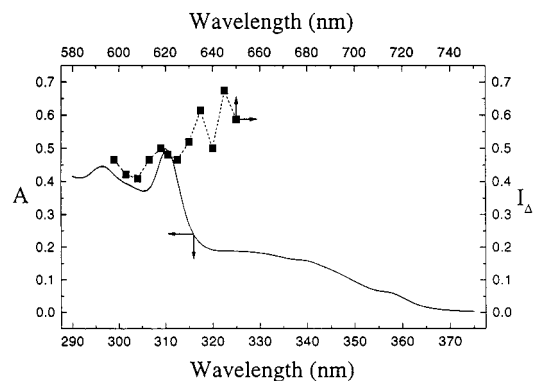


Figure 5. Plot of the normalized singlet oxygen phosphorescence intensity, I_A , against the irradiation wavelength for **Id** (top and right axes). Superimposed on this plot is the one-photon absorption spectrum of **Id** (bottom and left axes).

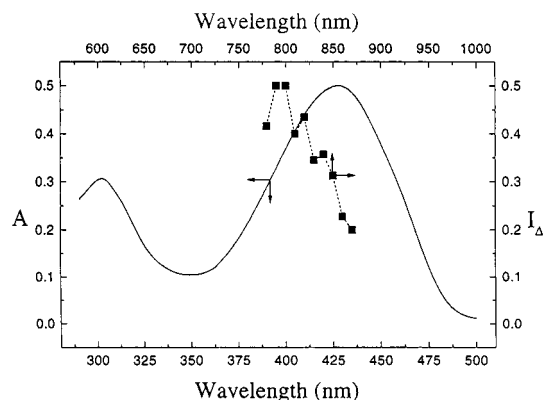


Figure 6. Plot of the normalized singlet oxygen phosphorescence intensity, I_A , against the irradiation wavelength for **II** (top and right axes). Superimposed on this plot is the one-photon absorption spectrum of **II** (bottom and left axes).

profiles likely reflect structure-dependent changes in the number of final states that can be accessed via a virtual state.

Although the preceding data are consistent with the production of singlet oxygen via a two-photon $S_0 \rightarrow S_n$ transition in the sensitizers **Ia–e** and **II**, it is important, for completeness, to consider other possible mechanisms of singlet oxygen production. For example, upon ~ 590 – 880 nm irradiation of our samples, singlet oxygen might be produced (a) from a charge-transfer (CT) state formed between oxygen and the abundant solvent molecules,²⁰ (b) upon an oxygen-enhanced $S_0 \rightarrow T_n$ transition in the sensitizer,²¹ and/or (c) upon excitation of oxygen itself.²² These alternative mechanisms can be discounted, however, on the basis of the following points. First, the induced $S_0 \rightarrow T_n$ transition is normally observed at oxygen pressures significantly greater than 1 atm, not in air-saturated samples at 1 atm.²¹ Second, if singlet oxygen were produced from an oxygen–toluene CT state or from a direct transition in oxygen, signal would have been observed in all instances, including from the sensitizer-free solvent. We thus conclude that our data are the result of a two-photon $S_0 \rightarrow S_n$ pumping scheme in **Ia–e** and **II**.

(17) Chen, C. H.; McCann, M. P. *J. Chem. Phys.* **1988**, *88*, 4671–4677.

(18) Birge, R. R. *Acc. Chem. Res.* **1986**, *19*, 138–146.

(19) Birge, R. R. In *Ultrasensitive Laser Spectroscopy*; Klinger, D. S., Ed.; Academic Press, Inc.: New York, 1983; pp 109–174.

(20) Scurlock, R. D.; Ogilby, P. R. *J. Phys. Chem.* **1989**, *93*, 5493–5500.

(21) Evans, D. F. *J. Chem. Soc.* **1957**, 1351–1357.

(22) Evans, D. F. *Chem. Commun.* **1969**, 367–368.

The singlet oxygen signals recorded upon two-photon irradiation of **Ia–e** and **II** were significantly smaller than signals typically recorded in a one-photon pumping scheme. For example, upon one-photon excitation of **Ib** with 355 nm irradiation at $<1 \text{ mJ pulse}^{-1} \text{ cm}^{-2}$, singlet oxygen signal-to-noise ratios of ~ 15 can routinely be recorded in our system using a single laser pulse. However, to record a signal-to-noise ratio of ~ 15 in the two-photon experiment where $I_L = 30 \text{ mJ pulse}^{-1} \text{ cm}^{-2}$ typically required the summation of data from ~ 1000 laser pulses. Moreover, in the two-photon experiments, it was necessary to discriminate between the singlet oxygen signal and a signal that originates as a consequence of the interaction between the solvent and the radiation field in the focused laser (e.g., Raman scattering and supercontinuum emission²³). In some cases, the latter signal can be sufficiently large as to saturate our detector. If the detector does not saturate, however, the decay of the undesired signal is limited by the response time of our system ($\sim 400 \text{ ns}$) and can be distinguished from the more slowly decaying singlet oxygen signal. The magnitude of this background signal at 1270 nm depends both on the solvent and on the irradiation wavelength. For example, this signal generally does not cause problems when focusing $\sim 600\text{--}800 \text{ nm}$ light into D_2O and toluene. On the other hand, in CCl_4 and CS_2 , the undesired signal can be appreciable.

Nanosecond Two-Photon Absorption Cross Sections.

Several experiments were done to assess the absolute as well as relative two-photon absorption cross sections in **Ia–d**. To describe this work, recall that both one- and two-photon pumping schemes will ultimately result in the formation of the lowest excited singlet state of the sensitizer, S_1 . Under conditions that preclude or minimize secondary absorption of light by the sensitizer within the irradiating pulse (i.e., low I_L , vide supra), the probability with which subsequent events occur will be independent of the mechanism by which S_1 was formed. Specifically, the efficiency of $S_1 \rightarrow T_1$ intersystem crossing and the efficiency with which ground-state oxygen quenches the sensitizer excited states to yield singlet oxygen will be identical in both the one- and two-photon pumping schemes. Thus, by normalizing the relative singlet oxygen intensities, I_Δ , obtained from the two-photon experiments by the corresponding one-photon singlet oxygen yield (Table 1), one should obtain a parameter proportional to the two-photon absorption cross section.

First, we note the absence of singlet oxygen signals upon $\sim 670\text{--}690 \text{ nm}$ irradiation of pyrene and acridine, for which two-photon cross sections of 0.22×10^{-50} and $2.0 \times 10^{-50} \text{ cm}^4 \text{ s photon}^{-1}$, respectively, have been measured at 694 nm .³ These values, which are small in comparison to values for molecules considered to be efficient two-photon absorbers,¹¹ allow us to estimate a lower limit for the two-photon cross sections in **Ia–d**. However, a better assessment of the two-photon absorption cross sections in **Ia–d** can be made by using compound **II** as a reference standard, for which a value of $(450 \pm 70) \times 10^{-50} \text{ cm}^4 \text{ s photon}^{-1}$ at 800 nm has been reported.¹¹

As shown in Figure 6, we find that compound **II** has a two-photon absorption maximum at $\sim 800 \text{ nm}$. Unfortunately, compound **II** does not have an appreciable two-photon cross section at $\sim 618 \text{ nm}$, for example, where **Ib** shows a nice maximum (Figure 4). Moreover, compounds **Ib** and **Id** do not have an appreciable two-photon absorption at 800 nm (i.e., singlet oxygen was not observed upon 800 nm irradiation of

Ib and **Id**). Thus, two-photon singlet oxygen signals recorded upon 800 nm irradiation of **II** must be compared to two-photon singlet oxygen signals recorded upon irradiation of **Ia–d** at a different wavelength and the data corrected for the respective photon energies. For solutions of **Id** and **II**, both at $3 \times 10^{-4} \text{ M}$, we find that **Id** has a two-photon absorption cross section at 618 nm that is ~ 2.2 times smaller than that of **II** at 800 nm . Relative 618 nm two-photon absorption cross sections in **Ia–d**, independently obtained, were then scaled accordingly (Table 1). Note that the smallest cross sections thus obtained, $(7\text{--}8) \times 10^{-50} \text{ cm}^4 \text{ s photon}^{-1}$ for **Ia** and **Ic**, are larger than the lower limit estimated for the cross sections using acridine (vide supra). The data in Table 1 indicate that the two-photon absorption cross sections for **Ia–d** are reasonably large and depend significantly on the nature of the substituent attached to the chromophore.

It is well established that two-photon absorption probabilities can depend on the relative polarization of the two photons that are simultaneously absorbed by the molecule.^{2,19} Such a polarization dependence, however, is not a requirement of a two-photon transition. In our experiment, we are able to control the relative polarization of the pumping photons such that their polarization axes are either parallel or perpendicular to each other (Figure 1). For all compounds examined, however, the intensities of the singlet oxygen signals observed upon irradiation were independent of the relative polarization of the light in the two irradiating optical paths.

Femtosecond Two-Photon Results. All of the experiments discussed thus far have been performed using a nanosecond laser as the irradiation source. It is well documented, however, that for two-photon experiments, there are many advantages to the use of a femtosecond laser as the irradiation source.⁶ The principal attribute of a much shorter irradiation pulse is the ability to deliver a comparatively high peak power and fluence using a comparatively small incident energy. Thus, two-photon transitions can be more readily pumped with significantly less photoinduced damage incurred by the system. Moreover, the repetition rate of a femtosecond system can be much greater than that of a typical nanosecond system, thus facilitating the process of signal averaging and the detection of weak emission signals. We thus felt it was important, in the least, to establish that singlet oxygen could likewise be detected in a two-photon photosensitized process using a femtosecond laser as the irradiation source.

Indeed, upon irradiation of compound **II** with a femtosecond laser at 802 nm in toluene ($\sim 1\text{--}50 \mu\text{J/pulse}$), we were readily able to observe singlet oxygen phosphorescence in a time-resolved experiment. As in the nanosecond experiments, it was necessary to discriminate between the singlet oxygen signal and a background signal arising from the laser–solvent interaction. Nevertheless, this was easily done, and appreciable singlet oxygen signal-to-noise levels (>20) were rapidly obtained ($<5 \text{ s}$) at a sampling frequency of 100 Hz . These data are consistent with the previously mentioned advantages of using a femtosecond laser to pump a two-photon transition.

Conclusions

We have demonstrated that time-resolved singlet oxygen phosphorescence can be detected from the small spatial domain of a focused laser beam after the two-photon excitation of a photosensitizer. In this work, a series of reasonably efficient two-photon singlet oxygen sensitizers were prepared. The singlet oxygen signals observed reflect the unique features of this nonlinear optical experiment: (1) depth penetration in the

(23) *The Supercontinuum Laser Source*; Alfano, R. R., Ed.; Springer-Verlag: New York, 1989.

sample afforded by irradiation in a spectral region void of the more dominant one-photon linear transitions and (2) spatial resolution afforded by irradiation with a focused laser beam. Thus, our results are significant with respect to two-photon pumping schemes in photodynamic therapy, a procedure where singlet oxygen can be a key reactive intermediate.²⁴ Our results are also pertinent with respect to the construction of a two-

photon emission microscope that can be used to create singlet oxygen images of heterogeneous materials.

Acknowledgment. This work was supported by grants from the Danish Natural Science Research Council and from the Council's initiative on Materials Research. The authors thank Søren Keiding and Jan Thøgersen for the use of, and assistance with, the femtosecond laser system.

(24) Fuchs, J.; Thiele, J. *Free Rad. Biol. Med.* **1998**, *24*, 835–847.

JA003468A